

Resolving large bed roughness elements with an unstructured hexahedral grid

N. R. B. Olsen

Department of Hydraulic and Environmental Engineering, The Norwegian University of Science and Technology, Trondheim, Norway

J. Aberle & Ka. Koll

Leichtweiß-Institut für Wasserbau, Technische Universität Braunschweig, Braunschweig, Germany

ABSTRACT: A three-dimensional numerical model is used to compute the water flow field in a straight flume with a cobble bed. The geometry of the numerical model is a replication of a physical model experiment where the largest cobbles were approximately 10 cm long. Detailed information on the digital terrain model of the bed was available from a laser scan of the bed. In the experiments, flow velocity profiles and turbulence properties were measured with a 3D-Laser Doppler Anemometer at 24 randomly selected locations. For the numerical simulations, the bed roughness is resolved with a very fine unstructured grid with dominantly hexahedral cells, adapted to the larger stones. At the bed, also a few tetrahedral cells are used. The unstructured grid allows for a varying number of grid cells in the vertical direction, depending on the water depth. The grid has 72 million cells, covering a flume area of 2.1 m in the longitudinal direction, 0.71 m in the width and 0.21 m over the depth. The cell sizes are smaller than 2 mm in the horizontal directions and smaller than 1 mm in the vertical direction. Results from the numerical model are compared with the flume measurements on the basis of the measured velocity profiles.

Keywords: Numerical models, Bed roughness, Hydraulic roughness, Velocity profile

1 INTRODUCTION

The turbulent flow and associated boundary layer in natural channels is strongly influenced by the roughness conditions on the channel bed. Compared to the homogeneous roughness structure of smooth and/or technical surfaces, the roughness structure of surfaces composed of natural sediments is spatially heterogeneous. The irregular nature of the surface affects the near bed flow and hence bed shear stress and energy loss. The latter determines the water surface slope and the corresponding water levels showing the importance of the adequate characterization of roughness for both the analysis of experimental data and numerical modeling studies.

In experimental investigations it is possible to investigate the effect of bed roughness on the turbulent flow field by analyzing measured velocity and turbulence data. Initiated by the pioneering work of Nikuradse (1933) tremendous progress has been made in understanding the effects of roughness on the mean wall-normal velocity distribution (see Jimenez, 2004 for a review). Furthermore, the Double-Averaging Methodology

(Nikora et al., 2007a, b and references therein) provides a theoretical background for interpretation of experimental and high resolution numerical flow data over rough surfaces.

However, high resolution numerical studies using Large Eddy Simulation (LES) or Direct Numerical Simulation (DNS) are cost intensive and are therefore not yet appropriate for practical applications in river engineering. Until today, most practical problems are tackled using one-, two-, or three dimensional numerical models (1D, 2D, 3D). So far, the application of such models has not significantly advanced the understanding of flows over rough beds because the effect of roughness must be accounted for by roughness functions determined empirically from experiments (e.g., Stoesser & Aberle, 2009).

For example, when the roughness elements are fairly small compared to the water depth and the grid cell sizes, the common and most valid approach is using a friction factor representing the influence of roughness. This is achieved by using a Manning or Chézy friction factor in most 1D and 2D models. On the other hand, a roughness length scale expressed in the dimension of length

(e.g., equivalent sand roughness k_s) is usually used in 3D models. The roughness length is a parameter in the wall law applied to compute bed shear stress. This approach was developed based on data from experiments in which sand particles were used as surface roughness. The particles were single sized and regularly spaced resulting in an even, quite smooth bed surface. Particle shape and orientation as well as varying heights of the bed elevation which appear for gravel bed surfaces and have an effect on the flow field (see Cooper et al., 2008) were not considered. Thus, using this approach it is not possible to account for the small scale roughness structure and grain orientation in most numerical studies. In fact, with the current available knowledge, roughness height mostly remains a calibration parameter in numerical modeling studies used to tune numerical model outputs to measured data (Morvan et al., 2008). A recent discussion of the meaning of roughness and its implementation in computational models is given in Morvan et al. (2008).

A further problem arises resolving the bed topography when the roughness becomes larger. If the stone sizes d on the bed correspond to at least 1/10 of the water depth h (i.e., $h/d < 10$), the roughness protrudes into the grid cells of a 3D numerical model. Some rivers have even larger roughness elements where the boulders protrude through the water surface. Thus, in such situations, it is difficult to compute the correct water flow field with a 3D-numerical model solving the Reynolds-averaged Navier-Stokes equations (RANS).

There basically exist two different approaches to solving the problems discussed above (Olsen & Stokseth, 1995). One method is to apply an immersed boundary method where the drag forces from the water on the stones are computed. This approach has been used in several studies, for example Olsen & Stokseth (1995), Fischer-Antze et al. (2001), and Zinke & Olsen (2008). In this method a drag formula is used with an empirical formula for the drag coefficient. One problem with this method is that the drag coefficient is uncertain and difficult to predict accurately. Another problem is that the method does not give a detailed picture of the flow around the roughness elements.

The second method is to resolve the roughness elements with a fine grid. This method, applied in the current study, can be useful where detailed information on the flow field around the stones is needed, for example in fish habitat studies. Another use for the method is to obtain information for further and more detailed studies of flow over rough beds. For example, using the pressure field, it is possible to directly compute the drag

and lift of the larger stones. Thereby, it would be possible to assess if the largest stones would be eroded or not. The main problem with resolving the roughness using this method is that an extremely fine grid has to be used, requiring substantial computational resources. The numerical method used to accomplish this is described in the following sections. The proposed method is validated by comparing the computed flow field with measured velocities by means of vertical profiles of the velocity component in main flow direction over a rough gravel bed.

2 EXPERIMENTAL DATA

The experimental data used to verify the numerical methods stem from experiments carried out in the laboratory of the Leichtweiß-Institut für Wasserbau, Technische Universität Braunschweig. The experiments, described in detail in Aberle & Koll (2004) and Aberle et al. (2008) were carried out in a 0.9 m wide, 20 m long, and 0.60 m high tilting flume.

In this paper, we use data from a single experiment which was carried out over a rough stable armor layer characterized by $d_0 = 0.0063$ m, $d_{16} = 0.0084$ m, $d_{50} = 0.0184$ m, $d_{84} = 0.044$ m, and $d_{100} = 0.064$ m, where d_{xx} denotes the grain size for which xx % of material (weight) has a smaller size.

The digital elevation model (DEM) of the bed was obtained by scanning the stable armor layer topography over a length of 2.4 m and a width of 0.716 m with an Optimes laser displacement meter within the test section which was located 9 m downstream of the flume inlet (see Figure 1 for DEM).

Longitudinal bed profiles were recorded with a sampling interval of $\Delta x = 1$ mm with a lateral spacing between profiles of $\Delta y = 4$ mm, and with a vertical precision of ± 0.1 mm. The different sampling intervals in x and y directions reflect the footprint of the sampling volume of the Optimes laser system (0.2 mm in flow direction and 4 mm in transverse direction). In total, 180 longitudinal profiles were recorded per surface scan. For the armor layer under investigation, the standard deviation of bed elevations $\sigma_z = 8.2$ mm and the geometric roughness height k_r , describing the distance from maximum to minimum elevation equals 62.5 mm (see Aberle & Nikora, 2006 for further analyses of the bed structure).

Flow measurements were carried out with a Dantec 3D-Laser Doppler Anemometer (LDA). For the presented data set, 24 randomly distributed vertical profiles of 3D velocities were measured with a sampling interval of 1 minute

and sampling frequencies > 20 Hz (see Figure 1 for positions). The measurements were carried out with immersed LDA-probes to enable flow velocity measurements within the roughness layer (Figure 2; see Aberle, 2006 for description of LDA-setup). The vertical sampling resolution of the velocity measurements was $\Delta z = 2$ mm below roughness tops, $\Delta z = 4$ mm above roughness tops, and $\Delta z = 10$ mm in the outer flow field. The measurements were carried out with a steady uniform discharge of $Q = 90.6$ l/s and a flume slope of $S = 0.027$. The mean water depth h , measured from mean bed elevation to water surface, corresponded to $h = 0.173$ m resulting in a relative submergence $h/k_r = 2.8$ ($h/d_{84} = 3.9$). Further information on the analysis of the data from all conducted experiments can be found in Aberle & Koll (2004), Aberle (2006) and Aberle et al. (2008).

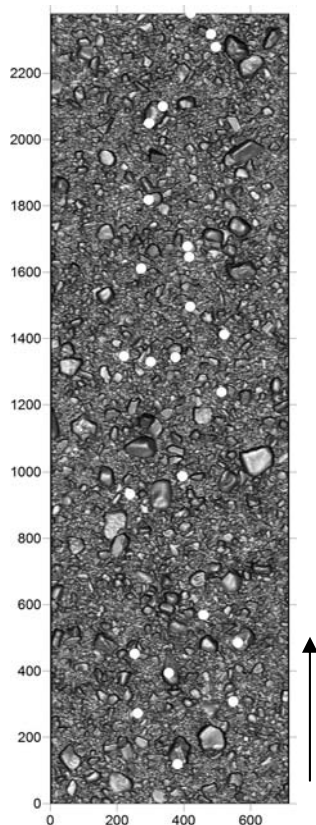


Figure 1. Digital elevation model of the armor layer shown as shaded relief map. The white dots indicate the randomly chosen LDA-measuring positions. Axis units are in mm.

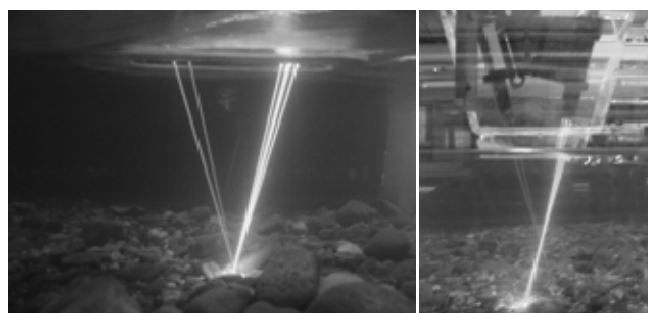


Figure 2. LDA-measurements in the roughness layer (left) and in the outer flow field (right).

3 NUMERICAL MODEL AND GRID GENERATION

The 3D numerical modelling approach used in this study is based on a very fine unstructured grid in order to resolve the bed roughness. The basis of the unstructured grid was a structured orthogonal 3D grid that covered both the water and the particles at the bed. The unstructured grid was made by removing the cells that were completely filled with solids, i.e., cells which were located below the bed elevations of the DEM. The cells above the surface were kept from the original orthogonal grid. The remaining cells were partially filled with water and partially filled with solids, i.e. contained the DEM surface. Shape changes were made for these cells by raising the bed elevations of the four bottom corners vertically up to the level of the DEM. Thereby only the water part of the cell was considered. This caused the bed cells to change in shape to become non-orthogonal. As the CFD code used in this study, SSIIM 2, was able to compute with non-orthogonal cells this was not a problem.

Some cells were located very close to the edge of a stone. In such cases, the angle between the grid line along the bed and the vertical grid line was sometimes very small. This led to very non-orthogonal cells, causing stability problems and inaccuracies. To avoid such grid cells, they were simply removed. The neighbouring cells were then left with no cells at their sides, creating vertical lines along the lower boundary of the grid. This can be seen in Figure 4 and 5 (at the end of the paper).

After this procedure, the new unstructured grid had been made with only the wetted cells. One advantage of the unstructured grid was that cells partially or fully containing solids were removed saving computational time. Moreover, such cells would require special immersed boundary techniques in the solution of the RANS-equations. When all the cells are only filled with water, such algorithms are not necessary. Another feature of the grid algorithm was that, since the original grid was orthogonal, only a very few cells close to the bed were non-orthogonal. Since the main flow direction followed the grid lines, false diffusion was thereby reduced.

A detailed example for the grid of the large roughness studied is displayed in Figures 4 and 5. As seen in the figures, non-horizontal grid lines are generated at the bed, allowing some of the sides of the hexahedral cells to be shorter than the others. Also, some sides may be shortened down to zero, allowing for tetrahedral cells close to the bed. This, together with the variable number of grid cells in the vertical direction, allows for re-

solving the larger stones in the bed. The resulting grid has 72 million cells, covering a flume area of 2.1 m in the longitudinal direction, 0.71 m in the width and 0.21 m over the depth.

The CFD code used in this study computed the water velocities by solving the RANS-equations in three directions. The SIMPLE method was used for computation of the pressure and the $k-\varepsilon$ model was used to resolve the Reynolds stresses. Rough wall laws with a relatively low roughness length of $k_S = 0.6$ mm were used at the bed as a consequence of the high grid resolution.

The main problem with the current case was the very long computational time due to the large number of grid cells. A solver for an unstructured grid is also usually much slower than for a structured grid. This problem was reduced by using a multi-grid solver which was only applied to the pressure-correction algorithm in SIMPLE. A multi-grid algorithm uses a mixture of fine and coarse grids to achieve a fast convergence. The coarse grid will transport changes in a variable faster across the domain than a fine grid. The current algorithm was originally made for natural rivers where the horizontal dimensions were much larger than the vertical direction. Therefore, the residuals from the pressure-correction equation were first summarized vertically on a depth-averaged grid. Then this grid was made incrementally coarser by joining four neighbouring cells into one. The procedure was repeated until the equation could be solved on a grid with only a few cells. The solution was transferred to the finer grid, solved again and so on until the original 3D grid had gotten its corrections.

To increase the computational speed, the program was also parallelized using OpenMP and running it on an IBM PowerPC cluster with 16 CPUs and 128 GB RAM on each node. The computational time for the 72 million cell grid was about two weeks running on one node. The RAM requirements were about 1 GB pr. 1 million cells.

One of the major problems in the calculation was to specify the upstream boundary condition for the velocities and turbulence parameters. In the current study, a logarithmic velocity profile was chosen for the velocities. Also, specified profiles of turbulent kinetic energy k and dissipation ε were used. However, the values of these profiles were unknown and thus they have an effect on the results adding some uncertainty.

4 RESULTS AND DISCUSSION

Figure 6 (at the end of the paper) shows the comparison of the results obtained from the numerical model and the measured velocity profiles. For the

comparison, only profiles at the central part of the computational domain were taken (one meter downstream the upstream boundary and 30 cm upstream of the downstream boundary). Avoiding the areas close to the upstream boundary reduced possible problems with the unknown inflow velocity and turbulence distributions. In fact, as the velocity profile and the turbulence parameters at the upstream boundary were not known, it was assumed that a length of about 1 m is required to develop the flow in the numerical model. In addition, the assumed logarithmic velocity profile contains a roughness parameter, which was set to 3 cm in the current study. There is a possibility that this may not be the correct value and that the upstream velocity profile is not completely logarithmic due to the influence of the upstream roughness structure.

In addition, the pre-defined upstream values of the turbulence parameters k and ε affect the turbulence in the main computational domain and the eddy-viscosity has also some effect on the velocity profiles. In this context it is worth mentioning that the comparison of computed and measured velocity profiles showed a poor agreement within the first downstream meter of the computational domain.

The downstream boundary conditions were zero-gradient for all variables resulting in a smaller impact of the downstream boundary compared to the inflow boundary. For this reason, only the three velocity profiles located at $x > 2200$ mm (Figure 1) were excluded from the analysis.

The comparison of the velocity profiles at single positions (Figure 6) shows a fairly good agreement between computation and measurement. Averaging the velocity profiles of the twelve presented positions also in the spatial domain (Figure 3) confirms the good agreement for the flow field above the roughness layer. However, measured and computed profiles deviate slightly below the roughness crest. The underestimation of the velocity by the calculation increases towards the bed.

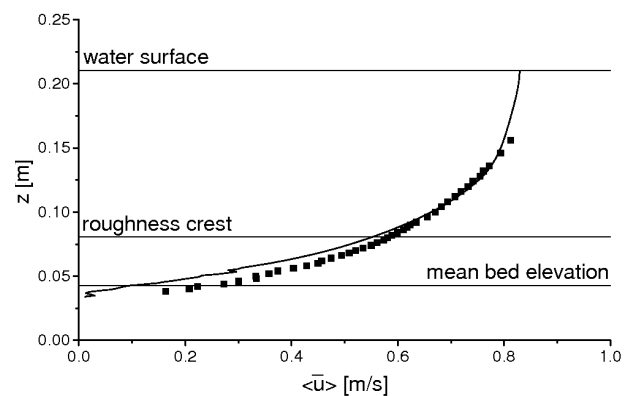


Figure 3. Double averaged vertical velocity profiles (solid line = computed profile, symbols = measured profile).

The slight deviation may be explained by the coarseness of the grid. Although the grid cells are less than 2 mm long and wide, the unevenness of the grid may be felt somewhat for the medium gravel. Another cause of error could be the roughness of the cobble surface. It was set to 0.6 mm, which was a reasonable value for most of the bed. However, some individual gravel particles may have had a smoother or rougher surface possibly affecting the velocity profile. A parameter study of the roughness could be included in further work. A third possible cause for the deviations may be that the grid does not capture subsurface water flow. It was thought that this effect would be small, but for some locations there might be an effect of this limitation in the grid.

One of the purposes of the current study was to investigate the possibility of computing cases with a large number of grid cells. A good multi-grid solver is then essential. The currently used algorithm had been very successful on grids in natural rivers, where only up to 20 cells were used in the vertical direction (Rüther et al., 2010). Using 100 000 cells, convergence was achieved in 2 ½ minute of computing time on a 16 processor IBM PowerPC cluster. However, when as many as 200 cells were used in the vertical direction, the algorithm did not perform optimally, as the first grid coarsening was based on depth-averaging. Preferably, the grid coarsening should have been done in all three directions simultaneously. The current runs took two weeks to converge. This problem did not affect the accuracy of the solution, though, only the computational time.

5 CONCLUSIONS

A method for computing the velocity field on a channel with rough bed by using a very fine unstructured body-fitted grid was presented. The large stones of the bed roughness are resolved directly in the grid, enabling a detailed computation of the velocity field near the bed. Comparing the measured velocity profiles and the computed values showed fairly good agreement.

Further studies on the case may include parameter tests on the skin roughness of the bed. Also, the upstream boundary condition for the velocity and turbulence quantities should be investigated. An option for improvements would be to use some kind of cyclic boundary condition. As the upstream and downstream cross-section of the grid is not completely similar, this is not straightforward due to the irregular nature of the bed surface. Some kind of averaging over the width may be used. Further research will be carried out along these lines.

ACKNOWLEDGEMENTS

The current study received computational time from the NOTUR programme, which is gratefully acknowledged. We also want to thank the staff at the high-performance cluster of the Norwegian University of Science and Technology for their assistance in compiling and running our program on the parallel machine. The laboratory experiments were carried with financial support of DFG (Deutsche Forschungsgemeinschaft) under contract DI-651/4-3.

REFERENCES

- Aberle, J. 2006. Spatially averaged near-bed flow field over rough armor layers. *Int. Conf. on Fluvial Hydraulics River Flow 2006*, Lisbon, Portugal, 153-162.
- Aberle, J., Koll, Ka. 2004. Double-averaged flow field over static armor layers. *Int. Conf. on Fluvial Hydraulics River Flow 2004*, Naples, Italy, Vol.1, 225-233.
- Aberle, J., Nikora, V. 2006. "Statistical properties of armored gravel bed surfaces." *Water Resour. Res.*, 42, W11414, doi:10.1029/2005WR004674.
- Aberle, J., Koll, Ka., Dittrich, A. 2008. Form induced stresses over rough gravel-beds. *Acta Geophysica*, 56(3), 584-600.
- Cooper, J.R., Aberle, J., Koll, Ka., McLelland, S.J., Murphy, B.M., Tait, S.J. Marion, A. 2008. Observation of the near-bed flow field over gravel bed surfaces with different roughness length scales. *Proc. River Flow 2008*, 3-5 September 2008, Cesme, Turkey. Kubaba, Vol. 1, 739-746.
- Fischer-Antze, T., Stoesser, T., Bates, P. Olsen, N.R.B. 2001. 3D numerical modelling of open-channel flow with submerged vegetation. *J. Hydraul. Res.*, 39(3), 303-310.
- Jiménez, J. 2004. Turbulent flows over rough walls. *Annu. Rev. Fluid Mech.*, 36, 173-196.
- Morvan, H., Knight, D., Wright, N., Tang, X., Crossley, A. 2008. The concept of roughness in fluvial hydraulics and its formulation in 1D, 2D and 3D numerical simulation models. *J. Hydraul. Res.*, 46(2), 191-208.
- Nikora, V., McLean, S., Coleman, S., Pokrajac, D., McEwan, I., Campbell, L., Aberle, J., Clunie, D., Koll, Ka. 2007. Double-Averaging concept for rough-bed open-channel and overland flows: Applications. *J. Hydraul. Eng.*, 133(8), 884-895.
- Nikora, V., McEwan, I., McLean, S., Coleman, S., Pokrajac, D., Walters, R. 2007b. Double-Averaging concept for rough-bed open-channel and overland flows: Theoretical Background. *J. Hydraul. Eng.*, 133(8), 873-883.
- Nikuradse J. 1933. Strömungsgesetze in rauhen Röhren, VDI-Forsch. 361 (Engl. transl. 1950. Laws of flow in rough pipes. NACA TM 1292).
- Olsen, N.R.B., Stokseth, S. 1995. Three-dimensional numerical modeling of water flow in a river with large bed roughness. *J. Hydraul. Res.*, 33(4), 571-581.
- Rüther, N., Jacobsen, J., Olsen, N. R. B. and Vatne, G. 2010. Prediction of the three dimensional flow field and bed shear stresses in a regulated river in Mid-Norway. Accepted to Hydrology Research.

Stoesser, T., Aberle, J. 2009. Turbulent open-channel flow over a gravel bed. 33rd IAHR Congress, 9-14 August 2009, Vancouver, Canada, papers on CD-Rom.

Zinke, P. Olsen N.R.B. 2007. Modeling of sediment deposition in a partly vegetated open channel. Proc. 32nd IAHR Congress, Venice, Italy, Papers on CD-Rom.

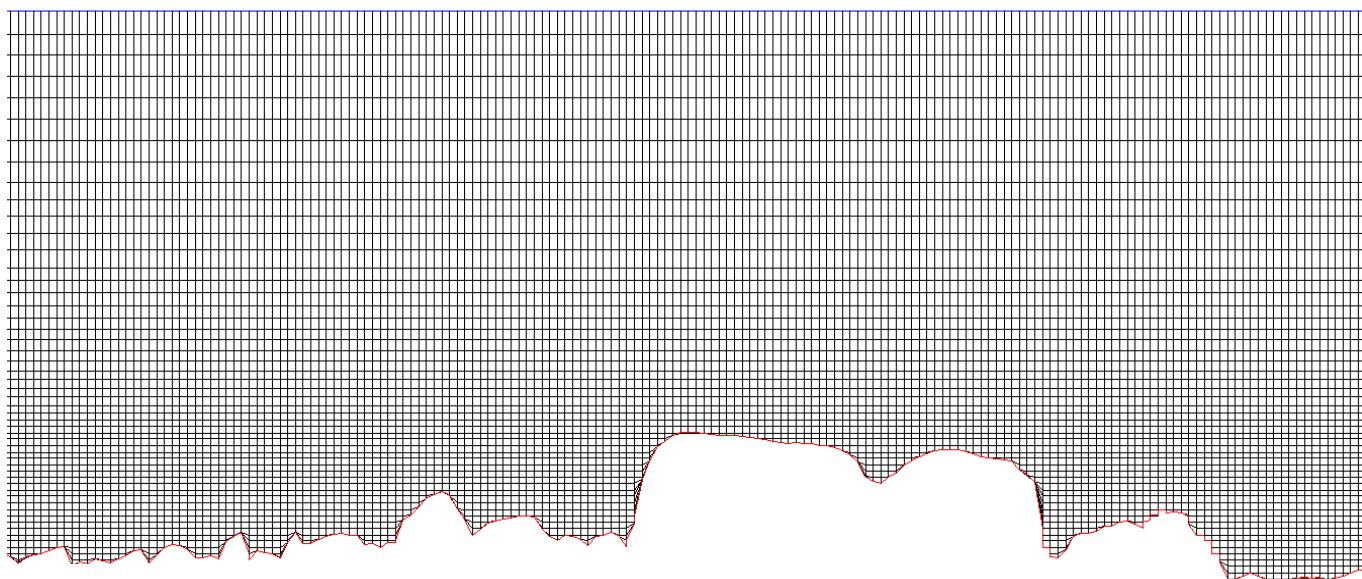


Figure 4. Part of a longitudinal section of the grid.

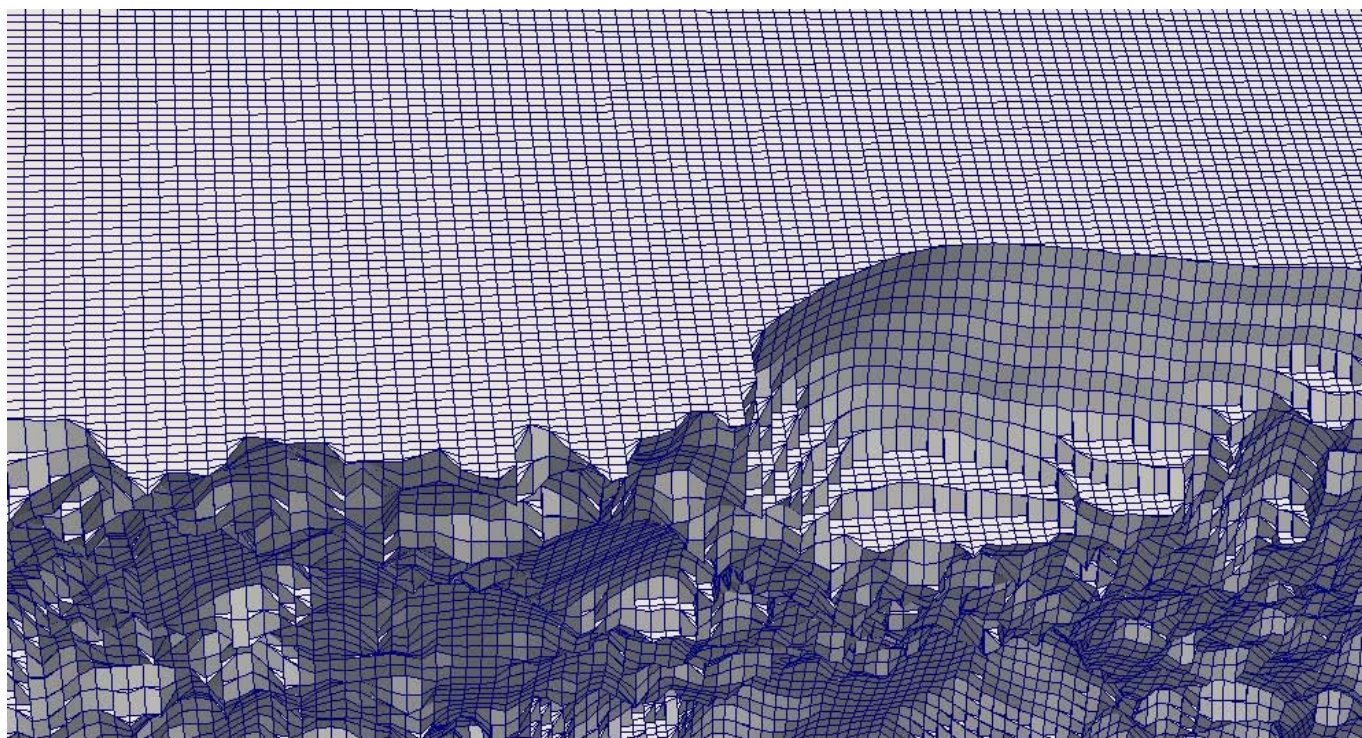


Figure 5. 3D view showing a section of the grid.

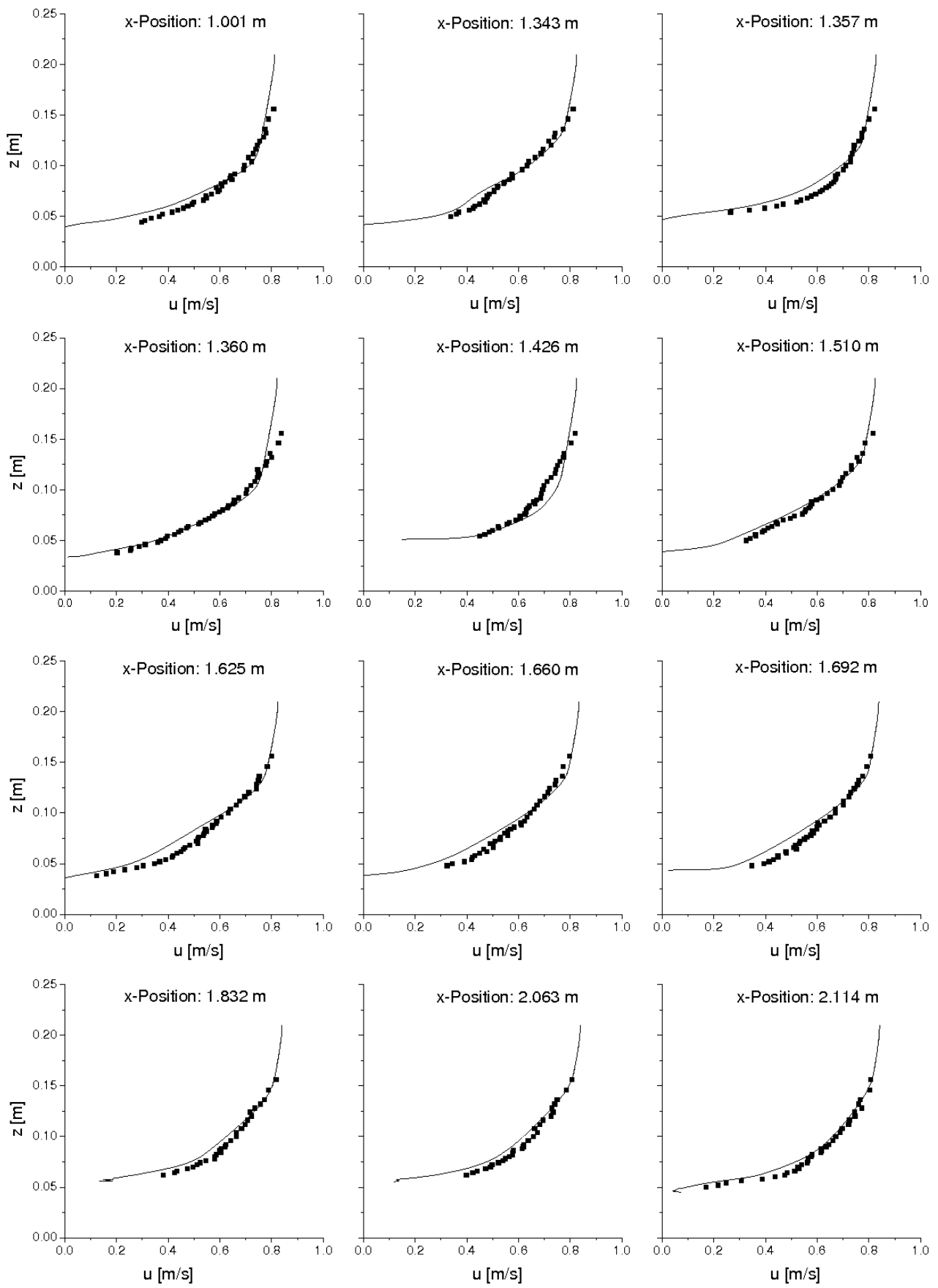


Figure 6. Vertical profiles of computed and measured velocities in the longitudinal direction. The squares are measurements and the solid lines are the results of the computations.